19 Molecular Plasma Membrane Dynamics Dissected by STED Nanoscopy and Fluorescence Correlation Spectroscopy (STED-FCS)

Christian Eggeling and Alf Honigmann

CONTENTS

19.1 INTRODUCTION

19.1.1 Molecular Interactions and Diffusion Dynamics in the Cellular Plasma Membrane

The cellular plasma membrane is built up by a lipid bilayer and contains a multitude of different lipids and proteins, which among other things play a central role in cellular signaling (Figure 19.1). It is well acknowledged that the different membrane molecules are highly dynamic but do not just simply diffuse freely as introduced in 1972 by the "fluid mosaic model."[1] Rather, molecular membrane diffusion is usually restricted and hindered; that is, it shows highly anomalous diffusion patterns and

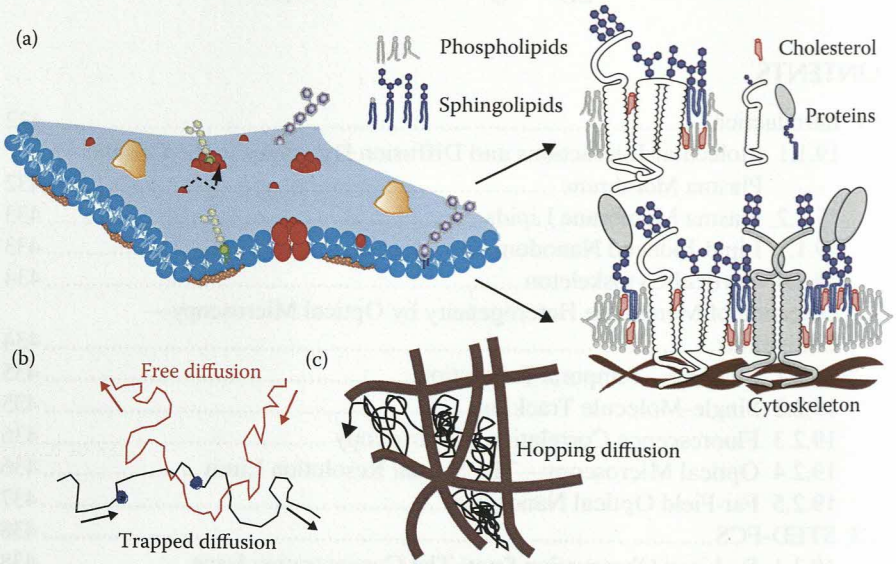

FIGURE 19.1 Plasma membrane heterogeneity. (a) Sources of membrane heterogeneity may be lipid–protein interactions, asymmetric molecular distribution to the leaflets, the underlying cytoskeleton (membrane anchored via proteins), and membrane curvature and pits. These heterogeneities result in hindered diffusion of lipids and proteins and may be the basis for the coalescence of transient signaling platforms—often denoted membrane domains or lipid rafts, spatially confined molecular assemblies of different lipids and proteins that are essential for a cellular signaling event. (Adapted from Lingwood, D., and K. Simons, *Science* 327 [2010]: 46–50.[2]) Hindered diffusion may be caused by (b) transient molecular interactions or incorporations into domains, which leads to an interruption or slowdown of diffusion, or (c) compartmentalization of the membrane, which causes a hopping diffusion.

only for a few molecules appears free, following free Brownian motion (e.g., Refs. 2 through 7) (Figure 19.1). For example, interactions with immobilized or slow-moving proteins lead to the local trapping of molecules, and the time to get from one point of the membrane to another is prolonged, especially on small spatial scales (e.g., Refs. 4 and 8). Similarly, the incorporation into putative domains of high molecular order leads to a local, transient slowdown (e.g., Refs. 2, 4 through 7, 9, and 10). Such slowdown may also stem from molecular crowding, since the mobility of molecules may already be retarded by the proximity to immobilized or relatively slow-moving molecules without direct interaction.[11] On the other hand, the influence of the cellular cytoskeleton, underlying the plasma membrane such as cortical actin, can be manifold. Proteins may transiently be arrested to the filament, thereby hindering their own mobility or, through interactions, the diffusion path of other molecules. Further, proteins that are anchored along the filament may be an obstacle for other diffusing molecules, acting like a picket or fence, and dividing the plasma membrane into compartments, whose boundaries may be hard to cross. As a consequence of this picket-fence model, molecules may show a kind of hopping diffusion with fast diffusion inside the compartments and hindered diffusion from one compartment to the next (see, for example, Refs. 3, 12, and 13). Therefore, diffusion may be fast on small spatial scales,[14] but extremely slowed down on long spatial scales.[4,10] Further, hindrances of molecular membrane motility may stem from obstacles such as membrane curvature or pits, induced by the cortical actin or proteins such as clathrin or caveolin (e.g., Refs. 15 through 17).

19.1.2 Plasma Membrane Lipids

Plasma membrane lipids have been acknowledged as a fundamental part of the functionality and regulation of integral or associated membrane proteins (e.g., Refs. 2, 7, and 18). This follows from novel experimental techniques and the recognition that membrane functionality is governed by the extremely high structural and chemical diversity of lipids and their highly heterogeneous spatiotemporal distribution.[19,20] It has been shown that specific lipid–protein interactions may induce conformational changes of proteins, thereby influencing the proteins' activity (e.g., Refs. 21 through 25). Lipids may, on the other hand, also be direct molecular receptors of, for example, viral particles or toxins, paving their way into or out of cells (for a review, see Refs. 2 and 7).

19.1.3 Lipid-Induced Nanodomains

An important feature of plasma membrane lipids is believed to be their ability to transiently bring together different proteins, thereby compartmentalizing cellular signaling events. Such signaling platforms are spatially localized and involve the tight packing of several proteins and lipids, and they are often referred to as membrane nanodomains or "rafts" (e.g., Refs. 2, 5 through 7, and 9) (Figure 19.1). The stabilization of such platforms may occur spontaneously or be triggered by extra- or intracellular events. While such nanodomains were initially believed to be stable,[6] they have recently be recognized as being of transient nature (e.g., Refs. 2 and 7). The higher local concentration of lipids and proteins may induce an increased molecular order, thereby resulting

in changes of the involved proteins' structure and functionality. Prominent examples of such platform-triggered processes include the modulation of cell growth,[26,27] the activation of lymphocytes such as T-cells,[28,29] viral uptake and budding such as of HIV,[19,30,31] or cellular internalization of molecules during endocytosis[32–37] (for an overview, see Refs. 2 and 7). In a lot of these cases, cellular signaling is governed by distinct lipid–protein interactions. For example, cellular uptake and thus toxicity of the cholera toxin is triggered by its binding to the ganglioside lipid GM1 (e.g., Refs. 33 and 37); similarly, GM1 acts as a receptor and thus initiator of internalization of the VP1 protein of the simian virus 40 (e.g., Ref. 36). Here, the binding affinity and, thus, the efficiency of the cellular uptake are influenced by both the multivalency of the binding (i.e., the necessity to simultaneously bind several GM1 lipids) and the lipid structure. It has been shown that the incorporation of these virus or toxins is most effective for saturated and long-chained GM1 analogues, while short unsaturated GM1 analogues hardly facilitate this process.[36] This observation supports the assumption that such processes are realized by domains of tight molecular packing (such as rafts), since long saturated lipids prefer areas of higher molecular order (e.g., Refs. 38 though 41).

Specifically, sphingolipids and membrane-associated cholesterol seem to play a central role in the formation of aforementioned signaling platforms. It has been shown several times that a lowering of the level of sphingolipids and cholesterol resulted in an interruption or disorder of cellular signaling processes (e.g., Refs. 2, 7, and 42 through 45).

Further, lipids are asymmetrically distributed to the inner and outer leaflet of the plasma membrane, thereby adding another cause for membrane heterogeneity. For example, certain phospholipids are rather found in the inner leaflet while sphingolipids such as gangliosides rather prefer the outer leaflet (e.g., see Ref. 46).

19.1.4 Cortical Cytoskeleton

Cytoskeleton structures such as microtubule, actin, or spectrin underlying the cellular plasma membrane play another central role in the membrane's bioactivity (Figure 19.1). Aforementioned hindrance of molecular mobility by proteins anchored to the cortical cytoskeleton (e.g., Refs. 3, 12, 47, and 48) may, on one hand, stabilize the lipid nanodomains or molecular clusters (e.g., Refs. 47 and 49) and, on the other hand, increase the interaction probability of less abundant molecules (e.g., Refs. 50 and 51). Another implication of the anchoring to the cortical cytoskeleton is that the plasma membrane cannot be considered as a planar layer.[17] The resulting membrane curvatures (e.g., at a local invagination such as clathrin-coated pits or caveolae) may be another cause of heterogeneous membrane organization and dynamics (e.g., Refs. 15, 17, and 52 through 55).

19.2 DETECTION OF MEMBRANE HETEROGENEITY BY OPTICAL MICROSCOPY—LIMITATIONS

Optical far-field microscopy has proven valuable for live-cell studies, since the use of focused light has proven to be minimally invasive (e.g., Ref. 56). Often, far-field

microscopy is combined with the fluorescence readout, where the studied molecule (e.g., a membrane protein or a lipid) is labeled with a fluorophore, and its fluorescence emission is excited, for example, by a laser and registered by a light detector. As a consequence, the position of a labeled molecule can be followed over space and time. In a confocal fluorescence microscope, a laser beam is focused to a small spot by an objective lens, which as well collects the emitted fluorescence and guides it onto a point detector. Scanning of the focused laser spot over the sample then allows reconstructing the spatial distribution of the fluorescently tagged molecules. Similarly, in wide-field microscopy, a larger area of the sample is illuminated at once and the spatial distribution of the fluorescence signal observed at once on a camera.

Molecular assemblies may be detected by spectroscopic techniques such as Förster resonance energy transfer (e.g., Refs. 18, 47, and 57) or by the use of fluorescent dyes that specifically label certain areas of the plasma membrane (e.g., Refs. 58 and 59). However, such experiments may be biased once they require an overexpression, that is, a very large concentration of the investigated molecules or membrane incorporation of the dyes, both of which may induce changes of the membrane.

19.2.1 Imaging—Temporal Resolution

A challenge is that most of the mentioned membrane heterogeneities are highly dynamic (such as the diffusing molecules), which makes the direct imaging of the heterogeneous distribution of fluorescently labeled molecules difficult.[57,60–64] On one hand, imaging techniques such as scanning confocal microscopy are usually too slow to follow these dynamics, such as the formation of transient domains. On the other hand, molecules have to be unevenly distributed between their free and bound state to be able to visualize molecular assemblies.[65] Many experiments, therefore, fix the cells and observe the state of a cell at a certain point of time. Unfortunately, fixation may result in artifacts or some membrane molecules might still be mobile after fixation.[66]

19.2.2 Single-Molecule Tracking

The direct observation of hindered diffusion of labeled molecules (instead of acquiring an instantaneous image) realizes a much better way of exploring membrane heterogeneity (e.g., see Refs. 3, 12, and 67). A prominent method is the spatiotemporal tracking of single isolated fluorescent molecules (single-molecule or single-particle tracking [SPT]): the emitted fluorescence signal is detected on a spatial sensitive detector such as a camera or several point detectors, and the molecule's position is determined over time with nanometer precision (e.g., Refs. 3, 12, 50, 51, and 67 through 70). Unfortunately, an accurate assignment of a diffusion mode, such as trapping versus hopping diffusion, is often not feasible.[71] Furthermore, SPT is a stochastic method, and either very long trajectories or a large number of short trajectories are required for a statistically relevant analysis,

which usually entails long and extensive measurement times. On the other hand, the recording of especially long trajectories as well as a high spatiotemporal resolution demands extremely bright and photostable fluorescent labels.[72] Therefore, SPT often employs large and bulky markers such as 20–40 nm large gold beads or 10 nm large quantum dots, which may themselves influence and thus bias the diffusion of the marked molecule.[73]

19.2.3 Fluorescence Correlation Spectroscopy

Methods such as fluorescence recovery after photobleaching (FRAP)[74,75] or fluorescence correlation spectroscopy (FCS)[4,76–79] usually require much shorter measurement times and small labels to acquire statistically relevant conclusions about the diffusion behavior of the investigated molecules. This follows from the fact that both techniques simultaneously observe the diffusion characteristics of a multitude of single molecules, which in SPT is only approximated by a large field of view or the use of photoswitchable fluorophores (e.g., Ref. 80). In FRAP, all fluorescent molecules within a micrometer-large area are photobleached (i.e., turned nonemissive) and the recovery of the fluorescence from this area is detected as nonphotobleached molecules diffuse into the area. The recovery curve allows the determination of diffusion coefficients and fractions of immobile species. Instead of photobleaching, one may also institute photoswitchable fluorescent labels.[81] In FCS, the temporal fluctuations of the observed fluorescence signal is monitored over time as molecules diffuse in and out of the observation area or volume (e.g., given by the micrometer-large focal laser spot of a confocal microscope[82]), and the correlation function of these fluctuations is calculated. The decay time of this correlation function usually renders the average transit time of the molecules through the observation area. Hindrances or anomalies in diffusion therefore result in a shift of the correlation curve toward larger times and the stretching of the decay.

19.2.4 Optical Microscopy—The Spatial Resolution Limit

The imaging or spectroscopic probing of molecular assemblies, or the probing of diffusion dynamics through FCS or FRAP on a far-field microscope, introduces a major limitation. Far-field optics introduce the diffraction of light, which limits the spatial resolution of such a lens-based microscope to approximately 200 nm for visible light.[83] As a consequence, a far-field microscope cannot distinguish alike molecules that are closer together than 200 nm and the structures below this size will appear blurred in the final image. In SPT, this issue is solved by detecting only single isolated (>200 nm apart) molecules and determining the central position of their blurred image spots. Because of the diffraction limit, FRAP and FCS experiments on a far-field microscope will average over nanoscopic hindrances in the diffusion characteristics.[8,65] A remedy to this issue has been suggested by spot-variation FCS (svFCS[4,8,84,85]), where correlation data are recorded for different sizes of the observation area above the diffraction limit. The resulting dependency of the average transit time through the observation spot allows more

detailed information of diffusion modes (free, trapping, or hopping diffusion). Using svFCS in 200 nm to >1 μm large observation areas, the diffusion characteristics of several different membrane lipids and proteins could be assigned to these modes.[10] Unfortunately, this assignment was only realized by an extrapolation to even smaller areas, and further details of the molecular dynamics such as a trapping period or area could only be estimated. Further, it cannot be ruled out that the extrapolation might be biased because of changes in the dependencies for observation areas smaller than the 200 nm diffraction limit. A remedy to all these limitations would be precise FCS measurements on the relevant scales, that is, with observation areas <200 nm. This has been facilitated by recording FCS data near nanometer-sized apertures, as for example realized by placing the membrane sample in zero-mode waveguides[86] or on a pattern of isolated nanoapertures milled in a metallic film,[87] or by placing a small tip with a nanometer-sized aperture near the sample (near-field microscopy).[88] Unfortunately, the collateral nanometer proximity of the sample to a surface might introduce unforeseeable bias. A more noninvasive way is the combination of FCS with subdiffraction far-field nanoscopy such as stimulated emission depletion (STED) nanoscopy (STED-FCS).[89,90]

19.2.5 Far-Field Optical Nanoscopy

Starting in the 1990s,[91] developments in optical microscopy have opened up the possibility to distinguish structures below the 200 nm diffraction limit with far-field optics (e.g., see Ref. 92). The key idea is to reversibly transfer the fluorescence markers between states of different emission properties, such as a dark and a bright state, thereby allowing the modulation or, reversibly, inhibition of fluorescence emission in space and time.[93–95] The first of such an optical nanoscope (or super-resolution microscope) was based on stimulated emission (STED) microscopy.[91,96] In a preferred implementation of STED nanoscopy, a laser is added to a conventional scanning (confocal) far-field microscope, which forces the fluorescent labels to their dark ground state, that is, inhibits fluorescence emission everywhere but at the center of the exciting laser focus (Figure 19.2). The wavelength of this second laser is tuned to the red edge of the fluorophore's emission spectrum and induces the stimulated de-excitation of the fluorophore's excited (and fluorescent) electronic (ON) to its ground (dark OFF) state. By detecting only the spontaneous (and not the stimulated) emission, the registered signal is efficiently decreased and completely switched off when increasing the intensity of the STED laser above a certain threshold (Figure 19.2). The introduction of a phase plate into the STED beam distorts its wave front and, once focused by the microscope objective, creates an intensity distribution that features one or several local zeros, such as a doughnut-shaped intensity distribution (Figure 19.2). However, while this intensity pattern is still ruled by diffraction, only an enhancement of the intensity of the STED laser drives the area in which fluorescence emission is still allowed to smaller and smaller subdiffraction scales. The spatial resolution of the STED microscope is therefore tuned by the intensity of the STED laser (Figure 19.2).

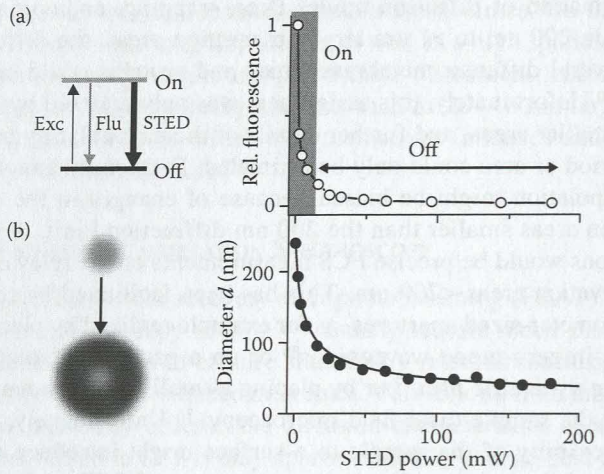

FIGURE 19.2 STED nanoscopy. (a) Optical nanoscopy relies on the transition between states of the fluorescent label with different emission characteristics. In the case of STED, these are the excited ON state, which is populated by the excitation laser (Exc) and which spontaneously depopulates by fluorescence emission (Flu), and the ground OFF state, to which the label is driven by (nondetected) stimulated emission using the additional STED laser. As a consequence, the STED laser inhibits spontaneous fluorescence emission. The efficiency of inhibition increases with the power of the STED laser, and the spontaneous fluorescence is efficiently switched off above a certain power threshold (right). (b) In a STED nanoscope, the diffraction-limited excitation (and thus fluorescence spot, gray) is overlaid with the STED laser, whose focal intensity distribution features at least one intensity-zero (black) (left). As a consequence, spontaneous fluorescence is inhibited everywhere but at the zero-intensity point, leaving a subdiffraction-sized area where emission is still allowed: the new observation spot, whose diameter d scales with the power of the STED laser (right).

19.3 STED-FCS

19.3.1 Reduced Observation Spot: The Concentration Issue

In conventional (confocal) FCS measurements, the average number of fluorescent molecules in the observation volume has to be kept rather low (<100–1000 depending on the signal-to-noise level), meaning that the concentration of fluorescently labeled molecules has to be kept low as well (<1 μM). This is however a concentration range that is often far below that of endogenous (biological) conditions. In contrast to measuring in zero-mode waveguides[86] or to photobleach[97] or switching off[98] large parts of the ensemble, the most obvious way to handle larger, endogenous concentrations would be lowering the observation spot's length scale.[99,100] Figure 19.3 shows FCS measurements of a fluorescent lipid analogue freely diffusing in a membrane on glass support. Switching from confocal (240 nm diameter of the observation spot) to STED recordings (60 nm diameter) clearly results in two effects:[89,90] (1) The average transit time through the observation spot, t_D, which correlates with the decay time of the FCS curve, decreases, as expected for a molecule following free Brownian

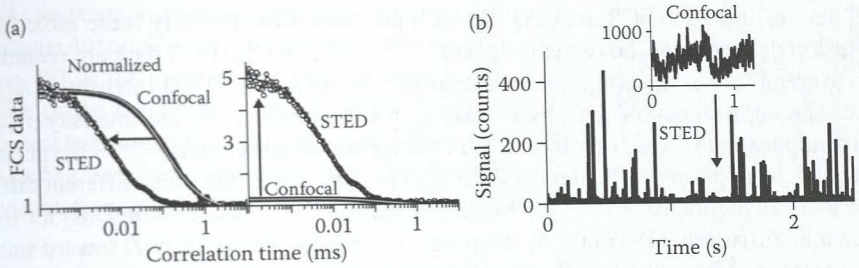

FIGURE 19.3 STED-FCS—reducing the observation spot. (a) STED-FCS analysis of free two-dimensional diffusion of a fluorescent lipid analogue in a multilamellar membrane. Representative correlation data (left, normalized amplitudes; right, original data) for confocal (black) and STED (60 nm) recordings (open dots). The confinement of the observation spot by STED reduces both the transit time and the average number of fluorescent molecules, leading to a shift of the correlation data to shorter correlation times (left) and an increase of the amplitude (right), respectively. (b) STED allows FCS-based single-molecule observations at high concentrations: fluorescence signal over time for the same concentration of a fluorescent lipid analogue diffusing in a multilamellar membrane indicates diffusion of single molecules only for the STED (right) but not for the confocal (left) recordings. (Adapted from Ringemann, C. et al., *New Journal of Physics* 11, 103054, 2009.)

diffusion; and (2) the average number, N, of fluorescent molecules in the observation volume, V, which changes inversely to the FCS curve's amplitude, decreases as well, as expected when lowering the observation volume but keeping the concentration ($c = N/V$) constant. As a consequence, much larger concentrations of fluorescently marked molecules can be used in measurements. For example, when moving from 240 nm large diffraction-limited to <50 nm large observation spots of the STED nanoscope, >25-fold concentrations (i.e., >20 μM) can in principle be employed for FCS measurements, as exemplified in Figure 19.3b, where clear fluctuations in the fluorescence signal caused by single-molecule transits (i.e., fluorescent bursts) can only be observed in the STED but not in the confocal recordings.

Similar to the aforementioned two-dimensional diffusion in a membrane, a shortening of the average transit time is equally well observed for three-dimensional diffusion when moving from diffraction-limited confocal to STED recordings.[89,90] While this makes STED-FCS measurements in solution or inside the cellular cytosol in principle feasible, these measurements are challenged by a lowered signal-to-background ratio owing to noninhibited out-of-focus fluorescence signal.[89,90]

19.3.2 Tuning of the Observation Spot: Studying Molecular Interactions

An important feature of the STED nanoscope for FCS is that the size of its observation spot can be tuned by the intensity of the added STED laser (Figure 19.2). One can use the principle of svFCS (compare previous discussions in Section 19.2.4[4,84,85]) and record and analyze FCS data at different sizes of the observation spot to determine the details of the hindrances in molecular diffusion. In contrast to the

diffraction-limited svFCS data, STED-FCS can now directly study these molecular diffusion dynamics at the relevant scales.[8,65,90,101,102] For this, FCS data are recorded and average transit times, t_D, were determined for different STED intensities, I_{STED}. Since the dependency of the observation spot's diameter, d, on the intensity, I_{STED}, can straightforwardly be obtained from calibration measurements,[8,101,102] the dependency of the apparent diffusion coefficient D ($\sim d^2/t_D$) on d discloses different diffusion modes (Figure 19.4):[101,102] (1) Normal diffusion: A constant value $D(d)$ for free Brownian diffusion. (2) Transient trapping: An ongoing decrease of D toward small d for a transient interaction with immobilized or slow-moving binding partners (slow relative to the interaction period). (3) Transient domain incorporation: A decrease of D toward small d but with a leveling off and even increase in values of D for spot diameters d smaller than the diameter of the domains.[103] (4) Hopping diffusion: An increase of D toward small d for the aforementioned cytoskeleton meshwork-based diffusion.[104] Even more, analysis of the STED-FCS data for $d < 80$–100 nm allows the determination of kinetic parameters, such as on and off rates of molecular complexes[8,65,90,101,102] or meshwork sizes and hopping probabilities.[105]

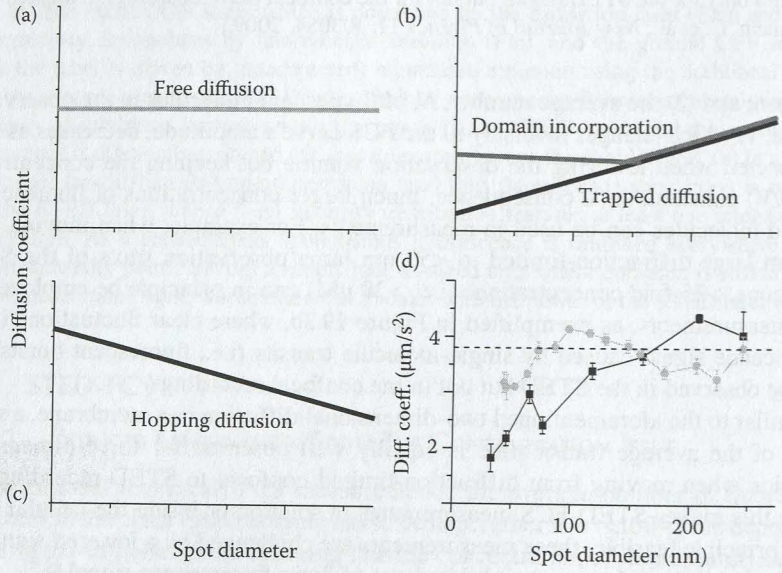

FIGURE 19.4 STED-FCS—observing diffusion modes by tuning the observation spot diameter. (a) Changing the STED power allows the determination of values of the apparent diffusion coefficient D for different diameters d of the observation spot. Sketched dependencies $D(d)$ for (a) free Brownian diffusion, (b) transient interaction with immobilized or slow-moving binding partners (transient trapping, black line) or transient domain incorporation (gray line), and (c) cytoskeleton meshwork-based hopping diffusion. (d) $D(d)$ dependency of the two-dimensional diffusion of a fluorescent lipid analogue in a fluid membrane bilayer on plasma-cleaned (gray circles) and non-plasma-cleaned (black squares) glass. Irregularities of the membrane bilayer by surface roughness and impurities may lead to a hindered diffusion in the case of the noncleaned glass substrate.

As an example, Figure 19.4b shows dependencies $D(d)$ recorded for a fluorescent lipid analogue diffusing in a fluid membrane bilayer on plasma-cleaned and noncleaned cover glass. While diffusion on the plasma-cleaned support was clearly free Brownian, diffusion on the noncleaned glass showed hindered diffusion, most probably attributed to transient trapping of the lipid analogues following irregularities of the membrane bilayer by surface roughness and impurities. Unfortunately, the transient trapping, that is, the deviation from normal diffusion, was too small to determine any kinetic parameters.

19.4 STUDYING LIPID–MEMBRANE DYNAMICS USING STED-FCS

19.4.1 Live-Cell Lipid Plasma Membrane Dynamics: Phospholipid versus Sphingolipid Diffusion

Figure 19.5 shows the dependency of the apparent diffusion coefficient $D(d)$ on the diameter d of the observation area (d = 30–240 nm) as determined from STED-FCS data recorded for two fluorescent lipid analogues in the plasma membrane of live mammalian cells: phosphoethanolamine (PE) and sphingomyelin (SM) labeled with

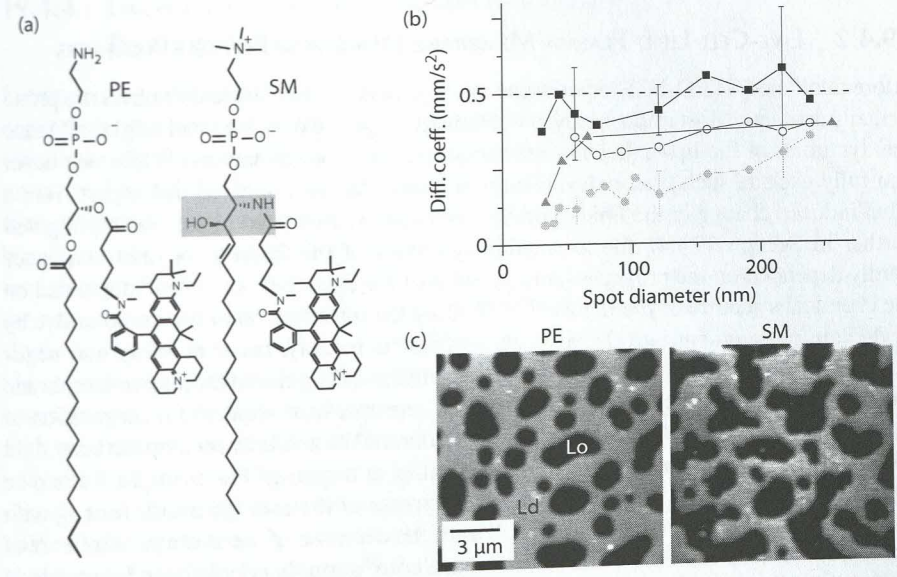

FIGURE 19.5 STED-FCS—lipid plasma membrane dynamics. (a) Structures of the fluorescent lipid analogues PE and SM both tagged with the organic dye Atto647N. Gray-shaded area: Ceramide or sphingosine group of the SM lipid. (b) Dependency of the apparent diffusion coefficient $D(d)$ on the diameter d of the observation spot for the diffusion of PE (black squares), SM (light gray circles), SM after cholesterol depletion (open circles), and SM after actin depolymerization (gray triangles) in the plasma membrane of live mammalian cells, indicating trapped cholesterol- and cytoskeleton-dependent diffusion of SM. (c) Comparison to phase separation in model membranes: both PE and SM hardly enter the liquid-ordered (Lo) domain, but rather prefer the liquid-disordered (Ld) domain of a model membrane bilayer composed of a ternary mixture[106] (confocal scanning fluorescence image; black, low signal; white, high signal).

the organic dye Atto647N.[8,65,90,101,102] These dependencies reveal an almost free diffusion of PE and a trapped diffusion of SM. A closer analysis of the FCS data for $d < 80$ nm revealed transient trapping of the lipids with on and off rates in the range of 190 s^{-1} and 800 s^{-1} for PE and of 80 s^{-1} and 80 s^{-1} for SM. While the fast on and off rates (equilibrium constant < 0.25) result in an almost normal diffusion of PE with a diffusion coefficient of ≈0.5 $\mu m^2/s$, the SM lipids are transiently arrested for approximately 10 ms on average every 10 ms (with a diffusion coefficient of ≈0.5 $\mu m^2/s$ every 200–300 nm).[90,101] The fact that the SM lipids hardly move during trapping indicates that they interact with other molecules such as membrane proteins, which are either relatively slow moving or even immobilized. It has to be pointed out that an accurate appointment of these on/off rates was impossible for diffraction-limited or even >60 nm large observation areas, even when interpolating to smaller scales.[90] Furthermore, the values of the on and off rates rendered an equilibrium constant of approximately 1 for SM; that is, at a certain point of time, 50% of all SM lipids were bound (and immobilized) and 50% were freely diffusing. As a consequence, there was no contrast between bound and unbound SM, and it is impossible to image this heterogeneous distribution of lipids, even with a STED nanoscope.[8,65]

19.4.2 Live-Cell Lipid Plasma Membrane Dynamics: Possible Artifacts

Aforementioned STED-FCS experiments on lipid plasma membrane dynamics are prone to many artifacts. Most importantly, the relatively large organic dye label might influence the dynamics of the lipid, thus not reflecting the true lipid dynamics. While one never can fully exclude such bias, extensive control experiments indicated that, apart from a label-induced change in the lipids' affinity for molecular ordered phases (as highlighted further in Section 19.4.4), the molecular dynamics of the fluorescent lipid analogues hardly depended on the properties and position of the dye label but instead depended on the chemical structure of the lipid.[8,101,102,107] Only the introduction of a very polar dye by acyl-chain replacement introduced biased diffusion, namely, faster mobility and negligible trapping (most probably from the polar label avoiding the hydrophobic membrane environment).[8] Further controls could rule out improper or nonspecific incorporation of the lipid analogues into the cellular plasma membrane[8,102] and influence by the laser light attributed to photobleaching, phototoxicity, heating, or trapping.[8] For example, it could be shown that—as expected from theory—the decrease of the average transit time t_D with increasing STED intensity coincided well with the decrease of the average number N of fluorescent molecules in the observation area, a correlation that could only be explained by the optically controlled decrease of the observation spot's length scale.[8] In the meantime, parts of the STED-FCS experiments could be confirmed by fast single-molecule tracking experiments,[70] as well as near-field microscopy observations.[88]

19.4.3 Live-Cell Lipid Plasma Membrane Dynamics: Molecular Dependencies

It could be shown that the molecular interactions of SM decreased upon treatment for cholesterol depletion (diffusion was almost free afterward, similar to PE), for

depolymerization of the underlying cellular cytoskeleton, and for lowering the level of endogenous SM (Figure 19.5). This indicated that either the binding interaction or the immobilization of the binding partner was assisted by cholesterol and SM and that most probably the binding partner was linked to the cytoskeleton.[8,101] Measurements at temperatures between 22°C and 37°C on the other hand revealed an Arrhenius-like dependency of the free diffusion coefficients but hardly any variation in trapping strength of SM.[101,102] The comparison of several different fluorescent lipid analogues, differing in their head group as well fatty acid chains, revealed lipid-specific dependencies of the lipids' molecular dynamics. Mainly, the ceramide (i.e., the NH and OH-) unit of the lipid backbone (gray in Figure 19.5a) was responsible for cholesterol- and cytoskeleton-dependent interactions, probably via hydrogen bonds. However, the polar head groups of, for example, ganglioside lipids such as GM1 induced transient binding as well, but less efficient and independent of cholesterol and the cytoskeleton.[101] In general, the interaction strength, frequency, and duration seemed very lipid specific, which points to specific and functional lipid–protein bindings.

19.4.4 Live-Cell Lipid Plasma Membrane Dynamics: Relation to Lipid Rafts

Summarizing aforementioned results, the observed cholesterol- and cytoskeleton-dependent interactions of the fluorescent SM sphingolipid are well described by transient (~10 ms long) binding to relatively immobile binding partners and only uncovered by STED-FCS. The >200 nm large diffraction-limited observation areas average over details on the nanoscale. The binding partners are most probably membrane proteins, whose mobility is restricted by the cytoskeleton. We can exclude that the lipids move during trapping; that is, it does not wander around inside a domain (or raft), where diffusion is slowed down. However, because the only dynamics of single molecules was observed, one cannot rule out the possibility that additional lipids or proteins molecules were (temporarily) included in this complex. However, the complex was not of very high molecular order, which was shown by a comparison with experiments on model membranes.[101,106,107] A model bilayer membrane of a ternary mixture of unlabeled saturated SM, unlabeled and unsaturated phosphoglycerolipids, and cholesterol separates into two different phases: a fluid liquid-disordered phase (Ld), which mainly includes the unsaturated lipids, and a liquid-ordered (Lo) phase and less fluid Lo phase of higher molecular order, which mainly includes the saturated lipid and cholesterol (e.g., see Refs. 38, 40, and 41). The Lo phase is often considered as a physical model system for membrane domains or rafts in the plasma membrane of living cells. The labeled SM analogue, however, did not partition into the Lo phase of this model system but favored the Ld phase (Figure 19.5b). Consequently, the lipid analogue was also not able to stain areas (or domains) of high molecular order in the plasma membrane, which were therefore missed by the previously mentioned STED-FCS experiments. Still, we can conclude that the observed strong interactions of the SM analogue were not driven by differences in molecular order; that is, the results of STED-FCS and phase separation experiments were not

correlated.[101,107] This is also exemplified by the fact that the fluorescent PE analogue partitioned similarly to the SM analogue but interacted much weaker with other constituents (Figure 19.5). Further, an elaborate study on a multitude of different lipid analogues using STED-FCS has shown that the partitioning characteristics of the analogue did not influence the transient trapping.[101,107]

It is possible that the interactions exposed by the STED-FCS experiments are those lipid–protein affinities that are the physicochemical basis of the coalescence of several molecules to the previously mentioned signaling platforms (or membrane rafts). However, it is unlikely that the investigation of this coalescence is possible with the presented fluorescent lipid analogues, since in comparison to the lipid, the rather large and often charged dye restricted the accessibility to highly ordered molecular assemblies such as the Lo phase or putative membrane rafts.[107] Nevertheless, it has been shown that the order of the Lo phase generated in cellular plasma membranes (which were treated by swelling procedures generating vesicular bilayers composed of native membranes such as giant plasma membrane vesicles[108] or plasma membrane spheres[109]) is much lower compared to model systems[110] and that more ordered phases of the plasma membrane are thus much more efficiently penetrated by the fluorescent lipid analogues.[107]

19.5 CONCLUSIONS

To investigate the discussed coalescence of potential signaling forms and existence of liquid-ordered nanodomains (or rafts) in the plasma membrane of living cells, it will be very important to study a functional fluorescent lipid analogue that does not alter phase partitioning and is compatible with STED-FCS, such as introduced recently.[103] First experiments using an Lo-partitioning fluorescent cholesterol analogue recently revealed fast and free diffusion of this probe, once again opposing a strong separation of model-membrane Lo-like domains in the plasma membrane of resting living cell.[111] It will therefore be very important to investigate lipid membrane dynamics after triggering of cellular functions including activation of different receptors.[2] Here, the development of two-color STED-FCS will allow relating lipid dynamics to changes in protein reorganization.[101] Scanning STED-FCS[112] or STED-RICS (raster image correlation spectroscopy),[113] as well as similar fluorescence fluctuation-based methods,[114] will highlight spatial heterogeneities in lipid diffusion.

At first, STED microscopy was realized with both the excitation and STED laser in a pulsed mode.[96,115] By letting the STED pulse swiftly follow the excitation laser, the fluorescence inhibition process is optimized, since the STED laser approaches the dye at the right point in time: in its excited state. STED microscopy, however, has also been realized with continuous-wave lasers,[116] an approach that has recently been significantly improved by the use of a gated detection scheme.[117,118] In this gated STED modality, the size of the observation spot (and thus the spatial resolution) can be tuned by both the power of the STED laser and the position of the gated detection window.[118,119] Gated STED-FCS has the potential to investigate temporal changes in lipid diffusion.[118]

STED-FCS is a sensitive and unique tool for studying nanoscale membrane organization and determining the cellular functions and molecular interdependencies

of membrane components. More generally, STED-FCS expands currently available optical microscopy and spectroscopy techniques to the nanoscale and opens up exceptional possibilities to characterize and disclose complex cellular signaling events and therefore new approaches for drug screening and development.[120]

ACKNOWLEDGMENTS

This work could not have been realized without the work of the people from the Department of NanoBiophotonics: Christian Ringemann, Veronika Mueller, Rebecca Medda, Vladimir Belov, Svetlana Polyakova, Birka Llaken, Class von Middendorf, and Andreas Schönle, especially by the extraordinary support and interaction with Stefan Hell, as well as by the lipid syntheses and discussions with Günter Schwarzmann (University Bonn). Further fruitful discussions with Herve Rigneault (Marseille), the Simons group (MPI Dresden), and the Schwille group (Bioquant Dresden) are greatly acknowledged.

REFERENCES

1. Singer, S., and G. L. Nicolson. "The Fluid Mosaic Model of the Structure of Cell Membranes." *Science* 175 (1972): 720–31.
2. Lingwood, D., and K. Simons. "Lipid Rafts as a Membrane-Organizing Principle." *Science* 327 (2010): 46–50.
3. Kusumi, A., C. Nakada, K. Ritchie et al. "Paradigm Shift of the Plasmamembrane Concept from the Two-Dimensional Continuum Fluid to the Partitioned Fluid: High-Speed Single-Molecule Tracking of Membrane Molecules." *Annual Review of Biophysics and Bioengineering* 34 (2005): 351–78.
4. Wawrezinieck, L., H. Rigneault, D. Marguet, and P. F. Lenne. "Fluorescence Correlation Spectroscopy Diffusion Laws to Probe the Submicron Cell Membrane Organization." *Biophysical Journal* 89 (2005): 4029–42.
5. Jacobson, K., O. G. Mouritsen, and G. W. Anderson. "Lipid Rafts: At a Crossroad between Cell Biology and Physics." *Nature Cell Biology* 9, no. 1 (2007): 7–14.
6. Simons, K., and E. Ikonen. "Functional Rafts in Cell Membranes." *Nature* 387 (1997): 569–72.
7. Simons, K., and M. J. Gerl. "Revitalizing Membrane Rafts: New Tools and Insights." *Nature Reviews Molecular Cell Biology* 11 (2010): 688–99.
8. Eggeling, C., C. Ringemann, R. Medda et al. "Direct Observation of the Nanoscale Dynamics of Membrane Lipids in a Living Cell." *Nature* 457 (2009): 1159–62.
9. Joly, E. "Hypothesis: Could the Signalling Function of Membrane Microdomains Involve a Localized Transition of Lipids from Liquid to Solid State?" *BMC Cell Biology* 5, no. 5 (2004): 3.
10. Lenne, P. F., L. Wawrezinieck, F. Conchonaud et al. "Dynamic Molecular Confinement in the Plasma Membrane by Microdomains and the Cytoskeleton Meshwork." *EMBO Journal* 25 (2006): 3245–56.
11. Niemela, P. S., M. S. Miettinen, L. Monticelli et al. "Membrane Proteins Diffuse as Dynamic Complexes with Lipids." *Journal of the American Chemical Society* 132 (2010): 7574–5.
12. Kusumi, A., Y. M. Shirai, I. Koyama-Honda, K. G. N. Suzuki, and T. K. Fujiwara. "Hierarchical Organization of the Plasma Membrane: Investigations by Single-Molecule Tracking vs. Fluorescence Correlation Spectroscopy." *FEBS Letters* 584 (2010): 1814–23.

13. Destainville, N., F. Dumas, and L. Salome. "What do Diffusion Measurements Tell us about Membrane Compartmentalisation? Emergence of the Role of Interprotein Interactions." *Journal of Chemical Biology* 1 (2011): 37–48.
14. Fujiwara, T., K. Ritchie, H. Murakoshi, K. Jacobson, and A. Kusumi. "Phospholipids undergo Hop Diffusion in Compartmentalized Cell Membrane." *Journal of Cell Biology* 157, no. 6 (2002): 1071–81.
15. Parton, R. G. "Caveolae—from Ultrastructure to Molecular Mechanism." *Nature Reviews Molecular Cell Biology* 4 (2003): 162–7.
16. Baumgart, T., B. R. Caparo, C. Zhu, and S. L. Das. "Thermodynamics and Mechanics of Membrane Curvature Generation and Sensing by Proteins and Lipids." *Annual Review of Physical Chemistry* 62 (2011): 483–506.
17. Adler, J., I. S. Andrew, P. Novak, Y. E. Korchev, and I. Parmryd. "Plasma Membrane Topography and Interpretation of Single-Particle Tracks." *Nature Methods* 7, no. 3 (2010): 170–1.
18. van Meer, G., D. R. Voelker, and G. W. Feigenson. "Membrane Lipids: Where They Are and How They Behave." *Nature Reviews Molecular Cell Bioliogy* 9 (2008): 112–24.
19. Brügger, B., B. Glass, P. Haberkant et al. "The HIV Lipidome: A Raft with an Unusual Composition." *Proceedings of the National Academy of Sciences of the United States of America* 103, no. 8 (2006): 2641–6.
20. Shevchenko, A., and K. Simons. "Lipidomics: Coming to Grips with Lipid Diversity." *National Reviews Molecular Cell Biology* 11 (2010): 593–8.
21. Bhushan, A., and M. G. McNamee. "Correlation of Phospholipid Structure with Functional Effects on the Nicotinic Acetylcholine Receptor." *Biophysical Journal* 64 (1993): 716–23.
22. Mantipragada, S. B., L. I. Horvath, H. R. Arias et al. "Lipid–Protein Interactions and Effect of Local Anesthetics in Acetylcholine Receptor-Rich Membranes from Torpedo Marmorata Electric Organ." *Biochemitry* 42, no. 30 (2003): 9167–75.
23. Fantini, J. "How Sphingolipids Bind and Shape Proteins: Molecular Basis of Lipid–Protein Interactions in Lipid Shells, Rafts and Related Biomembrane Domains." *Cellular and Molecular Life Sciences* 60 (2003): 1027–32.
24. Coskun, Ü., M. Grzybek, D. Drechsler, and K. Simons. "Regulation of Human EGF Receptor by Lipids." *Proceedings of the National Academy of Sciences of the United States of America* 108, no. 22 (2011): 9044–8.
25. Contreras, F.-X., A. M. Ernst, P. Haberkant et al. "Molecular Recognition of a Single Sphingolipid Species by a Protein's Transmembrane Domain." *Nature* 481 (2012): 525–9.
26. Bremer, E. G., J. Schlessinger, and S. Hakomori. "Ganglioside-Mediated Modulation of Cell Growth." *Journal of Biological Chemistry* 261, no. 5 (1986): 2434–40.
27. Kawashima, N., S.-J. Yoon, K. Itoh, and K. Nakayama. "Tyrosine Kinase Activity of Epidermal Growth Factor Receptor Is Regulated by GM3 Binding through Carbohydrate to Carbohydrate Interactions." *Journal of Biological Chemistry* 284, no. 10 (2009): 6147–55.
28. Zech, T., C. S. Ejsing, K. Gaus et al. "Accumulation of Raft Lipids in T-Cell Plasma Membrane Domains Engaged in TCR Signalling." *EMBO Journal* 28 (2009): 466–76.
29. Mahammad, S., J. Dinic, J. Adler, and I. Parmryd. "Limited Cholesterol Depletion Causes Aggregation of Plasma Membrane Lipid Rafts Inducing T Cell Activation." *Biochimica et Biophysica Acta (BBA)—Biomembranes* 1801 (2010): 625–34.
30. Chan, R., P. D. Uchil, J. Jin et al. "Retroviruses Human Immunodeficiency Virus and Murine Leukemia Virus Are Enriched in Phosphoinositides." *Journal of Virology* 82, no. 22 (2008): 11228–38.
31. Waheed, A. A., and E. O. Freed. "Lipids and Membrane Microdomains in HIV-1 Replication." *Virus Research* 143 (2009): 162–76.

32. Tsai, B., J. M. Gilbert, T. Stehle et al. "Gangliosides Are Receptors for Murine Polyoma Virus and SV40." *EMBO Journal* 22, no. 17 (2003): 4346–55.
33. Chinnapen, D. J. F., H. Chinnapen, D. Saslowsky, and W. Lencer. "Rafting with Cholera Toxin: Endocytosis and Tracking from Plasma Membrane to ER." *FEMS Microbiology Letters* 266 (2007): 129–37.
34. Römer, W., L. Berland, V. Chambon et al. "Shiga Toxin Induces Tubular Membrane Invaginations for Its Uptake into Cells." *Nature* 450 (2007): 670–5.
35. Hebbar, S., E. Lee, M. Manna et al. "A Fluorescent Sphingolipid Binding Domain Peptide Probe Interacts with Sphingolipids and Cholesterol-Dependent Raft Domains." *Journal of Lipid Research* 49, no. 5 (2008): 1077–89.
36. Ewers, H., W. Römer, A. E. Smith et al. "GM1 Structure Determines SV40-Induced Membrane Invagination and Infection." *Nature Cell Biology* 12 (2009): 11–8.
37. Wernick, N. L. B., D. J. F. Chinnapen, J. A. Cho, and W. Lencer. "Cholera Toxin: An Intracellular Journey into the Cytosol by Way of the Endoplasmic Reticulum." *Toxins* 2, no. 3 (2010): 310–25.
38. Bacia, K., D. Scherfeld, N. Kahya, and P. Schwille. "Fluorescence Correlation Spectroscopy Relates Rafts in Model and Native Membranes." *Biophysical Journal* 87 (2004): 1034–43.
39. Bagatolli, L. A. "To See or Not to See: Lateral Organization of Biological Membranes and Fluorescence Microscopy." *Biochimica et Biophysica Acta* 1758, no. 10 (2006): 1541–56.
40. Baumgart, T., G. Hunt, E. R. Farkas, W. W. Webb, and G. W. Feigenson. "Fluorescence Probe Partitioning between Lo/Ld Phases in Lipid Membranes." *Biochimica et Biophysica Acta* 1768, no. 9 (2007): 2182–94.
41. Marsh, D. "Cholesterol-Induced Fluid Membrane Domains: A Compendium of Lipid-Raft Ternary Phase Diagrams." *Biochimica et Biophysica Acta* 1788, no. 10 (2009): 2114–23.
42. Brown, D. A., and E. London. "Structure and Function of Sphingolipid- and Cholesterol-Rich Membrane Rafts." *Journal of Biological Chemistry* 275, no. 23 (2000): 17221–4.
43. Hao, M. M., S. Mukherjee, and F. R. Maxfield. "Cholesterol Depletion Induces Large Scale Domain Segregation in Living Cell Membranes." *Proceedings of the National Academy of Sciences of the United States of America* 98, no. 23 (2001): 13072–7.
44. Pike, L. J. "Rafts Defined: A Report on the Keystone Symposium on Lipid Rafts and Cell Function." *Journal of Lipid Research* 47 (2006): 1597–8.
45. Wüstner, D., L. Solanko, E. Sokol et al. "Quantitative Assessment of Sterol Traffic in Living Cells by Dual Labeling with Dehydroergosterol and Bodipy-Cholesterol." *Chemistry and Physics of Lipids* 164 (2011): 221–35.
46. Mondal, M., B. Mesmin, S. Mukherjee, and F. R. Maxfield. "Sterols Are Mainly in the Cytoplasmic Leaflet of the Plasma Membrane and the Endocytic Recycling Compartment in Cho Cells." *Molecular Biology of the Cell* 20, no. 2 (2009): 581–8.
47. Goswami, D., K. Gowrishankar, S. Bilgrami et al. "Nanoclusters of GPI-Anchored Proteins Are Formed by Cortical Actin-Driven Activity." *Cell* 135, no. 6 (2008): 1085–97.
48. Chichili, G. R., and W. Rodgers. "Cytoskeleton–Membrane Interactions in Membrane Raft Structure." *Cellular and Molecular Life Sciences* 66 (2009): 2319–28.
49. Machta, B. B., S. Papanikolaou, J. P. Sethna, and S. L. Veatch. "Minimal Model of Plasma Membrane Heterogeneity Requires Coupling Cortical Actin to Criticality." *Biophysical Journal* 100 (2011): 1668–77.
50. Andrews, N. L., K. A. Lidke, J. R. Pfeiffer et al. "Actin Restricts FcεRI Diffusion and Facilitates Antigen-Induced Receptor Immobilization." *Nature Cell Biology* 10, no. 8 (2008): 955–63.
51. Jaqaman, K., H. Kuwata, N. Touret et al. "Cytoskeletal Control of CD36 Diffusion Promotes Its Receptor and Signaling Function." *Cell* 146 (2011): 593–606.

52. Anderson, R. G. W., and K. Jacobson. "A Role for Lipid Shells in Targeting Proteins to Caveolae, Rafts, and Other Lipid Domains." *Science* 296 (2002): 1821–5.
53. Cheng, Z.-J., R. D. Singh, D. L. Marks, and R. E. Pagano. "Membrane Microdomains, Caveolae, and Caveolar Endocytosis of Sphingolipids (Review)." *Molecular Membrane Biology* 23, no. 1 (2006): 101–10.
54. Reynwar, B. J., G. Illya, V. A. Harmandaris et al. "Aggregation and Vesiculation of Membrane Proteins by Curvature-Mediated Interactions." *Nature* 447 (2007): 461–4.
55. Hatzakis, N. S., V. K. Bhatia, J. Larsen et al. "How Curved Membranes Recruit Amphipathic Helices and Protein Anchoring Motifs." *Nature Chemical Biology* 5 (2009): 835–41.
56. Pawley, J. B. *Handbook of Biological Confocal Microscopy*, 2nd ed. New York: Springer, 2006.
57. Hancock, J. F. "Lipid Rafts: Contentious Only from Simplistic Standpoints." *Nature Reviews. Molecular Cell Biology* 7 (2006): 457–62.
58. Parasassi, T., E. K. Krasnowska, L. Bagatolli, and E. Gratton. "Laurdan and Prodan as Polarity-Sensitive Fluorescent Membrane Probes." *Journal of Fluorescence* 8, no. 4 (1998): 365–73.
59. Kucherak, O. A., S. Oncul, Z. Darwich et al. "Switchable Nile Red-Based Probe for Cholesterol and Lipid Order at the Outer Leaflet of Biomembranes." *Journal of the American Chemical Society* 132 (2010): 4907–16.
60. Munro, S. "Lipid Rafts: Elusive or Illusive?" *Cell* 115 (2003): 377–88.
61. Lommerse, P. H. M., H. P. Spaink, and T. Schmidt. "In Vivo Plasma Membrane Organization: Results of Biophysical Approaches." *Biochimica et Biophysica Acta* 1664 (2004): 119–31.
62. Shaw, A. S. "Lipid Rafts: Now You See Them, Now You Don't." *Nature Immunology* 7, no. 11 (2006): 1139–42.
63. Groves, J. T., R. Parthasarathy, and M. B. Forstner. "Fluorescence Imaging of Membrane Dynamics." *Annual Review of Biomedical Engineering* 10 (2008): 311–38.
64. Pike, L. J. "The Challenge of Lipid Rafts." *Journal of Lipid Research* 50 (2009): S323–8.
65. Eggeling, C. "Sted-Fcs Nanoscopy of Membrane Dynamics." In *Fluorescent Methods to Study Biological Membranes*, edited by Y. Mely and G. Duportail, 291–309. Berlin: Springer-Verlag, 2012.
66. Tanaka, K. A. K., K. G. N. Suzuki, Y. M. Shirai et al. "Membrane Molecules Mobile Even after Chemical Fixation." *Nature Methods* 7 (2010): 865–6.
67. Lagerholm, B. C., G. E. Weinreb, K. Jacobson, and N. L. Thompson. "Detecting Microdomains in Intact Cells Membranes." *Annual Reviews Physical Chemistry* 56 (2005): 309–36.
68. Schutz, G. J., H. Schindler, and T. Schmidt. "Single-Molecule Microscopy on Model Membranes Reveals Anomalous Diffusion." *Biophysical Journal* 73 (1997): 1073–80.
69. Nishimura, S. Y., M. Vrljic, L. O. Klein, H. M. McConnell, and W. E. Moerner. "Cholesterol Depletion Induces Solid-Like Regions in the Plasma Membrane." *Biophysical Journal* 90 (2006): 927–38.
70. Sahl, S. J., M. Leutenegger, M. Hilbert, S. W. Hell, and C. Eggeling. "Fast Molecular Tracking Maps Nanoscale Dynamics of Plasma Membrane Lipids." *Proceedings of the National Academy of Sciences of the United States of America* 107, no. 15 (2010): 6829–34.
71. Wieser, S., M. Moertelmaier, E. Fuertbauer, H. Stockinger, and G. Schutz. "(Un) Confined Diffusion of CD59 in the Plasma Membrane Determined by High-Resolution Single Molecule Microscopy." *Biophysical Journal* 92 (2007): 3719–28.
72. Thompson, R. E., D. R. Larson, and W. W. Webb. "Precise Nanometer Localization Analysis for Individual Fluorescent Probes." *Biophysical Journal* 82 (2002): 2775–83.

73. Clausen, M., and B. C. Lagerholm. "The Probe Rules in Single Particle Tracking." *Current Protein and Peptide Science* 12 (2011): 699–713.
74. Yechiel, E., and M. Edidin. "Micrometer-Scale Domains in Fibroblast Plasma-Membranes." *Journal of Cell Biology* 105, no. 2 (1987): 755–60.
75. Feder, T. J., I. Brust-Mascher, J. P. Slattery, B. A. Baird, and W. W. Webb. "Constrainted Diffusion or Immobile Fraction on Cell Surfaces: A New Interpretation." *Biophysical Journal* 70 (1996): 2767–73.
76. Magde, D., W. W. Webb, and E. Elson. "Thermodynamic Fluctuations in a Reacting System—Measurement by Fluorescence Correlation Spectroscopy." *Physical Review Letters* 29, no. 11 (1972): 705–8.
77. Ehrenberg, M., and R. Rigler. "Rotational Brownian Motion and Fluorescence Intensity Fluctuations." *Chemical Physics* 4, no. 3 (1974): 390–401.
78. Fahey, P. F., D. E. Koppel, L. S. Barak et al. "Lateral Diffusion in Planar Lipid Bilayers." *Science* 195, no. 4275 (1977): 305–6.
79. Schwille, P., J. Korlach, and W. W. Webb. "Fluorescence Correlation Spectroscopy with Single-Molecule Sensitivity on Cell and Model Membranes." *Cytometry* 36 (1999): 176–82.
80. Manley, S., J. M. Gillette, G. H. Patterson et al. "High-Density Mapping of Single-Molecule Trajectories with Photoactivated Localization Microscopy." *Nature Methods* 5, no. 2 (2008): 155–7.
81. Lippincott-Schwartz, J., N. Altan-Bonnet, and G. H. Patterson. "Photobleaching and Photoactivation: Following Protein Dynamics in Living Cells." *Nature Cell Biology* 5 (2003): S7–14.
82. Widengren, J., and R. Rigler. "Ultrasensitive Detection of Single Molecules Using Fluorescence Correlation Spectroscopy." In *Bioscience*, edited by B. Klinge and C. Owman, 180–3. Lund: Lund University Press, 1990.
83. Abbe, E. "Beiträge zur Theorie des mikroskops und der mikroskopischen Wahrnehmung." *Archiv für Mikroskopische Anatomie* 9 (1873): 413–68.
84. Humpolickova, J., E. Gielen, A. Benda et al. "Probing Diffusion Laws within Cellular Membranes by Z-Scan Fluorescence Correlation Spectroscopy." *Biophysical Journal* 91, no. 3 (2006): L23–5.
85. He, H. T., and D. Marguet. "Detecting Nanodomains in Living Cell Membrane by Fluorescence Correlation Spectroscopy." *Annual Review of Physical Chemistry* 62 (2011): 417–36.
86. Levene, M. J., J. Korlach, S. W. Turner et al. "Zero-Mode Waveguides for Single-Molecule Analysis at High Concentrations." *Science* 299 (2003): 682–6.
87. Wenger, J., F. Conchonaud, J. Dintinger et al. "Diffusion Analysis within Single Nanometric Apertures Reveals the Ultrafine Cell Membrane Organization." *Biophysical Journal* 92, no. 3 (2007): 913–9.
88. Manzo, C., T. S. van Zanten, and M. F. Garcia-Parajo. "Nanoscale Fluorescence Correlation Spectroscopy on Intact Living Cell Membranes with NSOM Probes." *Biophysical Journal* 100 (2011): L08–10.
89. Kastrup, L., H. Blom, C. Eggeling, and S. W. Hell. "Fluorescence Fluctuation Spectroscopy in Subdiffraction Focal Volumes." *Physical Review Letters* 94 (2005): 178104.
90. Ringemann, C., B. Harke, C. V. Middendorff et al. "Exploring Single-Molecule Dynamics with Fluorescence Nanoscopy." *New Journal of Physics* 11 (2009): 103054.
91. Hell, S. W., and J. Wichmann. "Breaking the Diffraction Resolution Limit by Stimulated-Emission—Stimulated-Emission-Depletion Fluorescence Microscopy." *Optics Letters* 19, no. 11 (1994): 780–2.
92. Hell, S. W. "Far-Field Optical Nanoscopy." *Science* 316, no. 5828 (2007): 1153–8.

93. Hell, S. W., S. Jakobs, and L. Kastrup. "Imaging and Writing at the Nanoscale with Focused Visible Light through Saturable Optical Transitions." *Applied Physics A: Materials Science & Processing* 77 (2003): 859–60.
94. Hell, S. W. "Strategy for Far-Field Optical Imaging and Writing without Diffraction Limit." *Physics Letters. Section A: General, Atomic and Solid State Physics* 326, no. 1–2 (2004): 140–5.
95. Hell, S. W. "Microscopy and Its Focal Switch." *Nature Methods* 6, no. 1 (2009): 24–32.
96. Klar, T. A., S. Jakobs, M. Dyba, A. Egner, and S. W. Hell. "Fluorescence Microscopy with Diffraction Resolution Barrier Broken by Stimulated Emission." *Proceedings of the National Academy of Sciences of the United States of America* 97 (2000): 8206–10.
97. Moertelmaier, M., M. Brameshuber, M. Linimeier, G. J. Schutz, and H. Stockinger. "Thinning out Clusters While Conserving Stoichiometry of Labeling." *Applied Physics Letters* 87 (2005): 263903.
98. Eggeling, C., M. Hilbert, H. Bock et al. "Reversible Photoswitching Enables Single-Molecule Fluorescence Fluctuation Spectroscopy at High Molecular Concentration." *Microscopy Research and Technique* 70, no. 12 (2007): 1003–9.
99. Weiss, S. "Shattering the Diffraction Limit of Light: A Revolution in Fluorescence Microscopy?" *Proceedings of the National Academy of Sciences of the United States of America* 97, no. 16 (2000): 8747–9.
100. Blom, H., L. Kastrup, and C. Eggeling. "Fluorescence Fluctuation Spectroscopy in Reduced Detection Volumes." *Current Pharmaceutical Biotechnology* 7, no. 1 (2006): 51–66.
101. Mueller, V., C. Ringemann, A. Honigmann et al. "STED Nanoscopy Reveals Molecular Details of Cholesterol- and Cytoskeleton-Modulated Lipid Interactions in Living Cells." *Biophysical Journal* 101 (2011): 1651–60.
102. Mueller, V., A. Honigmann, C. Ringemann et al. "FCS in STED Microscopy: Studying the Nanoscale of Lipid Membrane Dynamics." In *Methods in Enzymology*, edited by S. Y. Tetin, 1–38. Burlington: Academic Press, Elsevier, 2013.
103. Honigmann, A., V. Mueller, S. W. Hell, and C. Eggeling. "STED Microscopy Detects and Quantifies Liquid Phase Separation in Lipid Membranes Using a New Far-Red Emitting Fluorescent Phosphoglycerolipid Analogue." *Faraday Discussion* 161 (2013): 77–89.
104. Mueller, V., PhD thesis, University Heidelberg, 2012.
105. Andrade, D. M., M. P. Clausen, J. Keller et al. "Lipids Are Compartmentalized at the Plasma Membrane by the ARP2/3-Dependent Cortical Actin Cytoskeleton." *Nature Structural Biology* (2014): submitted.
106. Honigmann, A., C. Walter, F. Erdmann, C. Eggeling, and R. Wagner. "Characterization of Horizontal Lipid Bilayers as a Model System to Study Lipid Phase Separation." *Biophysical Journal* 98, no. 12 (2010): 2886–94.
107. Sezgin, E., I. Levental, M. Grzybek et al. "Partitioning, Diffusion, and Ligand Binding of Raft Lipid Analogs in Model and Cellular Plasma Membranes." *Biochimica et Biophysica Acta (BBA)—Biomembranes* 1818 (2012): 1777–84.
108. Baumgart, T., A. T. Hammond, P. Sengupta et al. "Large-Scale Fluid/Fluid Phase Separation of Proteins and Lipids in Giant Plasma Membrane Vesicles." *Proceedings of the National Academy of Sciences of the United States of America* 104, no. 9 (2007): 3165–70.
109. Lingwood, D., J. Ries, P. Schwille, and K. Simons. "Plasma Membranes Are Poised for Activation of Raft Phase Coalescence at Physiological Temperature." *Proceedings of the National Academy of Sciences of the United States of America* 105, no. 29 (2008): 10005–10.
110. Kaiser, H.-J., D. Lingwood, I. Levental et al. "Order of Lipid Phases in Model and Plasma Membranes." *Proceedings of the National Academy of Sciences of the United States of America* 106, no. 39 (2009): 16645–50.

111. Solanko, M. L., A. Honigmann, H. S. Midtiby et al. "Membrane Orientation and Lateral Diffusion of BODIPY-Cholesterol as a Function of Probe Structure." *Biophysical Journal* 105 (2013): 2082–92.
112. Mueller, V., A. Honigmann, H. Ta et al. "Scanning STED-FCS Reveals Spatiotemporal Heterogeneity of Lipid Diffusion in the Plasma Membrane of Living Cells." *Proceedings of the National Academy of Sciences of the United States of America* (2013): submitted.
113. Hedde, P. N., R. M. Dorlich, R. Blomley et al. "Stimulated Emission Depletion-Based Raster Image Correlation Spectroscopy Reveals Biomolecular Dynamics in Live Cells." *Nature Communications* 4 (2013): 2093.
114. Digman, M. A., and E. Gratton. "Lessons in Fluctuation Correlation Spectroscopy." *Annual Review of Physical Chemistry* 62 (2011): 645–68.
115. Donnert, G., J. Keller, R. Medda et al. "Macromolecular-Scale Resolution in Biological Fluorescence Microscopy." *Proceedings of the National Academy of Sciences of the United States of America* 103, no. 31 (2006): 11440–5.
116. Willig, K. I., B. Harke, R. Medda, and S. W. Hell. "STED Microscopy with Continuous Wave Beams." *Nature Methods* 4, no. 11 (2007): 915–8.
117. Moffitt, J. R., C. Osseforth, and J. Michaelis. "Time-Gating Improves the Spatial Resolution of STED Microscopy." *Optics Express* 19, no. 5 (2011): 4242–54.
118. Vicidomini, G., G. Moneron, K. Y. Han et al. "Sharper Low-Power STED Nanoscopy by Time Gating." *Nature Methods* 8, no. 7 (2011): 571–3.
119. Vicidomini, G., A. Schoenle, H. Ta et al. "STED Nanoscopy with Time-Gated Detection: Theoretical and Experimental Aspects." *PLoS One* 8, no. 1 (2013): e54421.
120. Eggeling, C., L. Brand, D. Ullmann, and S. Jaeger. "Highly Sensitive Fluorescence Detection Technology Currently Available for HTS." *Drug Discovery Today* 8, no. 14 (2003): 632–41.